Qeios

Emergent Minkowski-like spaces of many-observers relational event universes

Oded Shor PhD,[1,3 #] * & Felix Benninger MD[1,2,3 #] & Andrei Khrennikov, PhD[4]

[1]Felsenstein Medical Research Centre, Petach Tikva, Israel; [2]Department of Neurology, Rabin Medical Centre, Petach Tikva, Israel; [3]Sackler Faculty of Medicine, Tel Aviv University, Tel Aviv, Israel; [4]Faculty of Technology, Department of Mathematics, Linnaeus University, Vaxjö, Sweden

Corresponding author (*):

Oded Shor, Felsenstein Medical Research Centre, Petach Tikva, Israel;

shor.oded@gmail.com

 # Equally contributing first authors

Email of all authors:

Oded Shor	shor.oded@gmail.com
Felix Benninger	benninger@tauex.tau.ac.il
Andrei Khrennikov	Andrei.khrennikov@lnu.se

Running title: Emergent Minkowski-like spaces of many-observers relational event universes

Key Words: p-adic numbers; dendrograms; dendrogramic holographic theory; causal structure; Minkowski space ; event-universe.

Ethical Publication Statement

We confirm that we have read the Journal's position on issues involved in ethical publication and affirm that this report is consistent with those guidelines.

Funding

This research did not receive any specific grant from funding agencies in the public, commercial, or not-for-profit sectors.

Availability of Data and Materials

Data sharing is not applicable to this article as no new data were created or analyzed in this study.

Conflicts of Interest

None of the authors has any conflict of interest to disclose.

Acknowledgements: Chana and Shlomo Chane-Laskin, Eliyahu Myara for intelligent discussion and support.

https://doi.org/10.32388/MMVEOF.2

Abstract. This paper is devoted to the event-observational modelling in physics and more generally natural science. The basic entities of such modelling are events and where space-time is the secondary structure for representation of events. The novelty of our approach is in using new mathematical picture for events universe. The events recorded by an observer are described by a dendrogram, a finite tree. The event dynamics is realized in the dendrogramic configuration space. In a dendrogram all events are intercoupled via the hierarchic relational structure of the tree. This approach is called Dendrogramic Holographic Theory (DHT). We introduce the causal structure on the dendrogramic space, like the causal structure on the Minkowski space-time. In contrast to the latter, DHT-emergent causality is of the statistical nature. Each dendrogram represents an ensemble of observers with same relational tree-representation of the events they measured/collected. Technically the essence of the causal modelling is in encoding dendrograms by real parameters and in this way transition to the real space-time. Then we proceed in the framework of information geometry corresponding to Hellinger distance and introduce a kind of light-cone in the space of dendrograms. The real parameter spaces discovered in our numerical analysis, while related to an ensemble of observers, primarily represent purely observer-subjective and observer-dependent knowledge of an observer about the universe. In that sense these spaces are inherently subjective. This is a step towards development of DHT-analog special relativity.

1. Introduction

1.1. Treelike representation of relational structure for observed events

Dendrogramic Holographic Theory (DHT) is a single postulate theory, developed in a series of studies [1–6]. This is a relational-event-observational approach to physics and more generally natural science [7,8]. The only postulate that drives all the theoretical consequences is that Leibnitz principle holds. Leibnitz principle [9] or principle of the identity of indiscernibles is usually formulated in a specific manner such that if, for every property F, object x has F if and only if object y has F, then x is identical to y, or in the notation of symbolic logic: $\forall\ F(Fx \leftrightarrow Fy) \rightarrow x = y$, namely: if x and y are distinct, at least one property that x has and y does not or vice versa can be found.

DHT is a theory of information about events collected by observers. If two observations of two events cannot be distinguished in any feature by a certain observer these two events are the same event (by Leibnitz principle) to that observer.

For a some observations of a set of events, the observer needs to ask a series of questions in order to distinguish the observed events one from each other. The simplest form of questions are yes/no questions (but any p number of answers is possible). Mathematically these series of questions can be represented as trees (which can be understood as decision trees) which we call dendrograms. An observer can quantify the relation between two events as the first question, where the answer is not the same.

Within the context of an infinite number of events, the ontic description of the events is portrayed as an infinite tree. One class of such trees is p-adic trees, which are homogeneous trees with p > 1 edges branching from each vertex. These trees possess an algebraic structure and a topology consistent with this structure [10].
The p-adic topology is governed by the p-adic ultrametric, satisfying the strong triangle inequality. Consequently, this field is endowed with a strange geometry in that all triangles are isosceles. The p-adic distance between two branches of the tree is determined by their common root, where a longer common root (equivalent to more questions answered with same answer) signifies a shorter distance. Moreover, upon defining "open" and "closed" balls as:

$$B_{-}(R;a) = \{x : r_p(a,x) < R\}, B(R;a) = \{x : r_p(a,x) \leq R\}$$

Where $r_p(a,x) = |a-x|_p$ is the p-adic distance between the points a and x.

As branches represent (distinguished) events, the space of events, whether finite or infinite, is equipped with a p-adic ultrametric. In this way DHT is connected with p-adic analysis and theoretical physics [11–26] (including studies of Parisi et al [25] on complex disordered systems in the p-adic and more generally ultrametric framework; see also article [26]). General trees are endowed with ultrametric topology and such topological spaces were widely used in theory of complex disordered systems [15,27].

The main consequence of endorsing the Leibnitz principle is the need to distinguish events by the above-mentioned questions procedure. This procedure in turn is represented naturally by the p-adic number field. From this question procedure, represented as a p-adic tree, emerges immediately the relationship of each event to all other events. Thus, Leibnitz principle leads directly to Machian relationism, not as an assumpsion (in contrast to theories like shape dynamics and Brans-Dicke theory [28–30]) but as an inherent consequence of the p-adic tree representation of events. Moreover, endorsing Leibnitz principle leads to a background-independent theory similarly to theories like shape dynamics, loop quantum gravity, spin foams and causal set theory [28,29,31–33].

1.2. Coupling to Rovelli's relational quantum mechanics

We emphasize that DHT is neither quantum nor classical, these two paradigms emerge quite naturally from the p-adic relational tree as was shown in [1–3,5] with no extra assumption but that Leibnitz Principle holds. It is worth noting Rovelli's Relational quantum mechanics [34] (RQM) is very close ideologically to DHT, but postulates all systems are quantum systems. Similarly to DHT, RQM makes use of the fact that any quantum mechanical measurement can be reduced to a set of yes–no questions. It uses this fact to formulate the state of a quantum system (relative to a given observer! Same as in DHT). In contrast to DHT, RQM postulates the completeness of quantum mechanics. Thus, RQM postulates there are no hidden variables or other factors which may be appropriately added to quantum mechanics in light of current experimental evidence. As shown in [5] quantum theory can be considered as an emergent theory of a relational structure. Thus, completeness

is non-relevant as well as other factors such as hidden-variables. In that sense the different interpretations of quantum mechanics may be viewed as corresponding to different emergence schemes of quantum theory from an event relational structure. In RQM there are also two empirical postulates. These two empirical postulates are the following ones:

Postulate 1: *there is a maximum amount of relevant information that may be obtained from a quantum system*.

By omitting the quantum system postulate, DHT similarly agrees that the maximal amount of information about an event is encoded in the event branch contained in the ontic infinite p-adic tree.

Postulate 2: *it is always possible to obtain new information from a system*.

Similarly, by adding more events to the relational structure more information is gained to each of the events.

We emphasize that the RQM postulates turn to be just consequences of the relational structures.

1.3. Coupling to Smolin's approach to emergence of quantum mechanics

We note also Smolin's work on emergence of quantum mechanics and spacetime by introducing rationalism perspectives (for example energetic causal set theory and [35–38]) . Again these works are similar in ideology, but their construction stems from concepts like momentum, energy and even coordinates which are completely absent in the construction of DHT, but, again, can emerge out of the relational p-adic structure.

We also point out to some similarities between our approach leading to emergence of quantum theory from DHT and the neural network model of universe developed in articles [39–43].

1.4. Observer-dependent subjective knowledge of universe

In DHT two (or more) observers can have different epistemic views of the universe they observe (different relational structures). On the other hand two (or more) observers can have the same epistemic views of the universe although they observed different events (meaning these two observers have equal the inter-relations of the events they measured). In that sense the observer always has a subjective view of the universe, regardless of the universe classical or quantum nature. This aligns with *Bohr's principle of complementarity and event physics.* Bohr repeatedly stated that outcomes of physical observables are not objective properties of systems, but generated in the process of a measurement. On the other hand, the observer dependent view of the universe is also aligned with special relativity. Where a measurement of some event in spacetime is dependent on the observer (momentary) inertial frame.

If we characterize an observer as its world line curve (accelerated or not) on the background of spacetime, each observer will ultimately obtain different ontic relational view

of the universe (two observers with same world line are not allowed as they are the same observer if we postulate Leibnitz principle). This view is dependent on the information about events, localized in the background of spacetime, transmitted to the observer moving with acceleration or without it in
spacetime

Thus, information on the universe is strictly observer-dependent. In the DHT framework, measurements can be "subjective" in the sense of quantum mechanics and/or observer-dependent in the sense of special relativity, but both lead to a subjective knowledge of the universe.

In the present work we further explore the dynamical laws of subjective knowledge acquired by observers on a system, or universe. Our aim is to bring closer the event-observational approach with the principles of spacetime physics of special relativity. In order to accomplish that aim, we need to construct some spacetime model that will uniquely define a certain subjective relational-informational view of the universe. Moreover, such spacetime should possess a causal structure similar to the light-cone of the Minkowski spacetime.

DHT is not just an abstract theoretical construction. It is directly coupled to experiment: the experimental data of any origin is transferred into a dendrogram with the aid of clustering algorithms. Temporal dynamics of data-collection by an observer is represented as dynamics in the configuration space of dendrograms (see articles [1–3,7,8] for handling of concrete experimental data within DHT, especially article [4] devoted to the dynamics). This is the good place to remark that DHT is "invariant to using of different clustering algorithms'', in the sense that general properties of dynamics do not depend on an algorithm (although dendrogramic picturing can differs). For simplicity, we proceed with 2-adic, yes-no, clustering algorithms generating homogeneous 2-adic trees, with one incoming and two leaving branches for each vertex. We note that homogeneous trees can be endowed with algebra leading to the number field (or ring) structure.

1.5. Causal structure

In this paper we introduce the causal structure on the dendrogramic configuration space, like the causal structure on Minkowski space-time. However, in contrast to the latter, DHT-emergent causality is of the statistical nature. So, this is causality on the dendrogramic parameter space where each point in this parameter space represents an ensemble of observers with same epistemic dendrogramic, relational, representation of the events they measured/collected (subjective knowledge-view of the universe). We emphasize that the same dendrogram structure can be obtained for variety of measurement data. In fact, different measurement data-sets produce the same epistemic description of the universe when the relations between measurements are the same for different measurement data-sets.

In DHT, each observer generates his own event-dendrograms evolving in the configuration space. Transition from one point-dendrogram to another is also observer's

dependent. So, the DHT-causal structure is determined by ensembles of observers. In this way, we introduce the timelike and spacelike separated event-dendrograms.

Technically the essence of the causal modelling is in encoding dendrograms by real parameters and in this way transition to the real space-time, i.e., in the complete accordance with event mechanics, events are primary, and space-time is secondary.

Following the construction of the dendrogramic parameter space, we can introduce the information geometry causal structure. Thus, we consider the information metric on the space of probability distributions based on the Hellinger distance. This information metric determines a dendrogramic "light cone", which draws an analogy to the Minkowski spacetime metric that characterizes events. This concept allows us to analyze the propagation of information and observer interactions within the dendrogramic framework.

In this paper we perform an extended numerical simulation to check matching of the dendrogramic and real space representations as well as matching the corresponding notions of causality: in the dendrogramic space and four-dimensional Minkowski space-time.

The real parameter spaces discovered in our numerical analysis, while related to an ensemble of observers, primarily represent purely observer-subjective and observer-dependent knowledge of an observer about the universe. In that sense these spaces are inherently subjective.

We emphasize that DHT describes any kind of dynamics of experimental statistical data in the process of collection of outcomes of new observations performed by all possible observers. And it is surprising that any such process can be portraited in the Minkowski spac-time and its causal structure is consistent with the causal structure of special relativity.

2. Causal structure on the space of dendrograms corresponding to ensembles of observables

In our model, we introduce O_i $i=1,2,\ldots N\to\infty$ observers who collects/measures events/data. Thus an observer with already m events collected e_1, $e_2\ldots$ e_m will measure each time a single event, $e_{m+1.}$ Each time an observer O_i measures an event, he construct a dendrogram using the procedure outlined in appendix A1.

To represent the dendrogram, we utilize a series of p-adic numbers, with each number encoding the relationship of a single event to the remaining events acquired by the observers. It's important to note that a dendrogram can only be constructed when the number of events is greater or equal 2, as it relies on the relational structure among events.

Initially, all N observers have a trivial dendrogram with two branches.
As observers acquire more events, a range of potential dendrograms with three branches emerges. The number of observers (n) that generate a fixed, same, dendrogram can be

represented as a fraction out of all observers (N) in our universe n/ N. We note that in each **level** of m events collected contains all N observer and basically n=n(D) where D is a dendrogram. This iterative process allows the observers' dendrograms to evolve event by event, leading to increasingly complex relational structures. Please refer to Figure 3 for a visual representation.

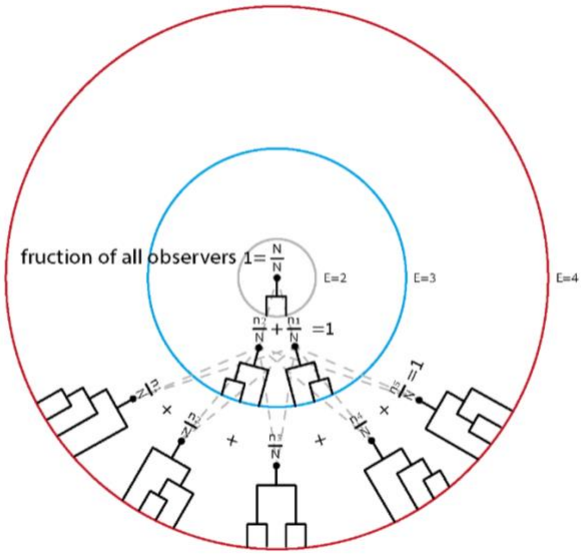

Figure 3: An Abstract Representation of the Dendrogram Space
This figure provides an abstract representation of the dendrogram space. At each level (E=2, 3, ..., M), unique dendrograms are displayed, with each one associated with a specific fraction of the N observers present in the universe. It is noteworthy that the cumulative fraction of observers' dendrograms at each level precisely sums up to 1, illustrating the complete representation of the entire observer population. In each level E=2,3..M each unique dendrogram belongs to a fraction of the N observers present in the universe. Each level total fraction of observers dendrograms sum to 1

a given dendrogram might have some dendrograms they can evolve to and some they will not. This is the case if a fraction of the observers with dendrogram D1 evolves to a dendrogram D2 other wise D1 does not evolve to D2. By examining the structure of two dendrograms, can we predict whether they are connected? Dendrograms that exhibit observer flow from one to the other can be referred to as "timelike separated" dendrograms, while dendrograms that show no observer flow between them can be classified as "spacelike separated". More specifically, "timelike/spacelike separated" dendrograms are defined as follows:

Definition 1. *D1 and D2 are two,* ***timelike separated****, different dendrograms with number of events/data collected* $e1 \leq e2$ *,respectively, if and only if there exist at least one observer with D1 dendrogram with* $e1$ *events moves from D1 to D2 upon collecting the next* $e2 - e1$ *events*

Definition2. *D1 and D2 are two,* ***spacelike separated****, different dendrograms with number of events/data collected* $e1 \leq e2$ *,respectively,*
if and only if there is no possibility for observers with D1 dendrogram with $e1$ *events to move from D1 to D2 upon collecting the next* $e2 - e1$ *events*

In essence, we introduce the concept of a dendrogramic "light cone,"
Definition 3. A specific dendrogram D is identified with numerous observers who share identical relations among all the observations each of them has made of the universe.

Thus a dendrogramic "light cone" is defined as

Definition 4. A dendrogramic "future light cone" associated with a particular unique dendrogram encompasses all the potential dendrograms that can emerge from dendrogram D. This holds true irrespective of the observer's identity in relation to D and takes into account all conceivable events and combinations of events they might measure.

This draws an analogy to the Minkowski spacetime metric that characterizes events. This concept allows us to analyze the propagation of information and observer interactions within the dendrogramic framework.

Please note that while the causal structure of Minkowski space is not statistical in nature, in DHT, we seek to establish a statistical counterpart referred to as the *"dendrogramic Minkowski causal structure of observers ensemble relational universes ".*
Where a *universe is defined as*

Definition 5. A universe is an observer, current, relational knowledge (information) he acquired on the ontic universe by measuring some finite amount of events

In this context, each dendrogram represents a fraction of observers who collect a specific number of events (e.g. level) this fraction of observers have same relations between their acquired events.

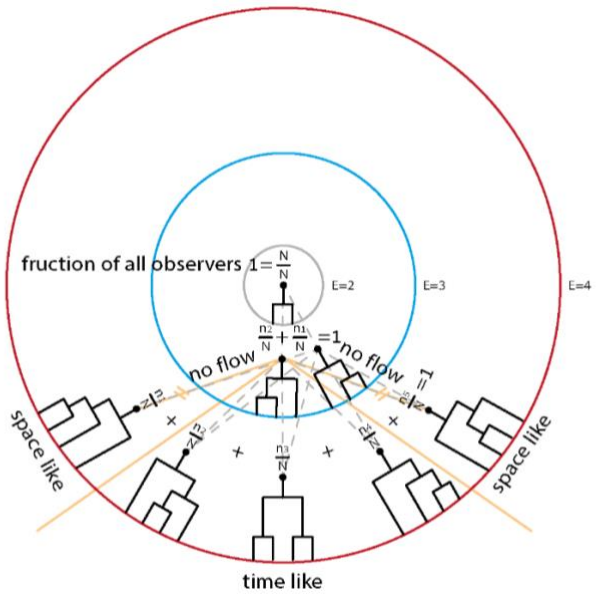

Figure 4: An Abstract Representation of the Causal Structure in the Dendrogram Space
This figure provides an abstract representation of the causal structure within the dendrogram space. Each dendrogram is characterized by a specific number of events, with one dendrogram containing E2

events located inside the lightcone of another dendrogram containing E1 events, where E2 is greater than E1. Remarkably, this relationship implies that at least one observer possessing the dendrogram with n1 events can transform it into the dendrogram with E2 events by collecting E2-E1 additional events. The illustration highlights the dynamic nature of the dendrogram space and its potential for causal transformations facilitated by event collection.

By discerning the relationships and connectivity patterns among dendrograms, we aim to gain insights into the causal connections and spatiotemporal dynamics within the observed events. Through this analysis, we can uncover the underlying structures that govern the flow of information about the universe (of the whole observer population up to the minimal fraction of the population) and the evolution of the observer's dendrograms.

In order to achieve this objective, we require a parameter space for dendrograms that uniquely characterizes each individual dendrogram. Remarkably, we demonstrate that such a parameter space can be obtained, and intriguingly, it manifests as a four-dimensional space. Additionally, we observe that the interval between any two dendrograms in this parameter space exhibits a signature akin to Minkowski spacetime—a combination of spacelike intervals with positive values and timelike intervals with negative values, or vice versa.

3. Real parametrization of dendrograms

In our study, we employed the following equation to facilitate our analysis: The representation of a dendrogram branch, denoted as $edge_i$, can be expressed as the sum of a series: $edge_i = \sum_{j=0}^{k} a_j \times 2^j, \quad a_j = 1,0$ *(1)*

where each term corresponds to the contribution of a specific level in the dendrogram's hierarchical structure. Here, a_j represents the binary digit at position j, with possible values of 0 or 1.

To further enhance our analysis, we introduce the concept of the monna map conversion. The monna map conversion of an event, denoted as $event_i$, is computed using the formula: $event_i = \sum_{j=0}^{k} a_j \times 2^{-j-1}$, $a_j = 1,0$.

(2)

where a_j represents the binary digits (0 or 1) in the 2-adic expansion of the dendrogram branch, and k is the maximum ball level of the dendrogram.

By applying this Monna map conversion, we represent events as rational numbers on the continuous interval [0, 1]. This conversion preserves the precise relations between events, ensuring that the inherent structure and ordering within the dendrogram branches are maintained. To quantify the differences between events, we introduced the metric q_{ik}, which represents the absolute difference between the monna map conversions of two events,

$q_{ik} = |event_i - event_k|$ *(3)*

Thus we can defined 5 elementary/fundamental parameters of a dendrogram

We define our dendrogramic vector, D , as follows:

$$E = event_i, i = 1,2 \ldots n = number\ of\ events$$

$$B = 2^{-maximal\ ball\ level\ of\ the\ dendrogram}$$

$$D = [E\ B]\ with\ elements\ D_i\ , i = 2,3 \dots n+1$$

$V_D = (\sum_{i=0}^{k} D_i\ )^z$

$U_D = (\sum_{i=0}^{k} \frac{1}{D_i + 1})^{z1}$

$M_D = (\sum_{i=1}^{k-1} \sum_{j=i+1}^{k} D_i \cdot D_j\ )^{z2}$

$R_D = (\sum_{i=1}^{k-1} \sum_{j=i+1}^{k} D_i - D_j\ )^{z3} = (\sum_{i=1}^{k-1} \sum_{j=i+1}^{k} q_{ij}\ ) + \sum_{j=i+1}^{k} |B - D_j|)^{z3}$

$$r_D = (\sum_{i=1}^{k-1} \sum_{j=i+1}^{k} 1/((D_i - D_j\ ) + 1))^{z4} =$$

$(\sum_{i=1}^{k-1} \sum_{j=i+1}^{k} 1/(q_{ij} + 1) + \sum_{j=i+1}^{k} 1/(|B - D_j| + 1))^{z4}$

$k = number\ of\ branches\ and\ thus\ events\ in\ dendrogram$ *(4)*

Where z,z1,z2,z3 and z4 each takes a random a value, in our numerical simulations *z,z1,z2,z3 and z4* (presented in section 6) will have, randomly, a value from *T=[-2 -1 -0.5 0.5 1 2]*

We then constructed from a combination of them another 55 parameters in the following way. 1. all possible two elementary parameters product combinations. Thus adding 10 more parameters

2. all possible two elementary parameters sum combinations. Thus adding 10 more parameters

3. all possible two elementary parameters division combinations. Thus adding 20 more parameters

4. all possible three elementary parameters product combinations. Thus adding 10 more parameters

5. all possible four elementary parameters product combinations. Thus adding 5 more parameters.

Overall, we have 60 possible parameters. These 60 parameters will be used for numerical deep scan of possible "dendrogramic Minkowski causal structure of observers ensemble"

4. dendrogramic parameter space

we will demonstrate now that there are parameters spaces that have the ability to uniquely define a unique dendrogram structure (this set of z, z1, z2, z3, z4 and parameters $\theta'_1\ , \theta'_2\ , \theta'_3\ and\ \theta'_4$ are the one shown as examples in figures 6 and 10) .

$$\theta'_1 = (U_D)^{-2}$$

$$\theta'_2 = (V_D)^{0.5}/(U_D)^{-2}$$

$$\theta'_3 = (U_D)^{-2}(V_D)^{0.5} {R_D}^{-0.5} (M_D)^2$$

$$\theta'_4 = \sqrt{n}(r_D)^2/{R_D}^{-0.5}$$

Lets suppose $\theta'_1 = \theta''_1\ , \theta'_2 = \theta''_2, \theta'_3 = \theta''_3\ and\ \theta'_4 = \theta''_4$ *for two different dendrograms* D' *and* D'' *then if* $\theta'_1 = \theta''_1$ *and* $\theta'_2 = \theta''_2$ *then* $(U_{D'})^{-2} = (U_{D''})^{-2}$ *and* $\frac{(V_{D'})^{0.5}}{(U_{D'})^{-2}} = \frac{(V_{D''})^{0.5}}{(U_{D''})^{-2}}$ *which means* $(V_{D'})^{0.5} = (V_{D''})^{0.5}$ *the combination*

$\begin{cases}(U_{D\prime})^{-2} = (U_{D\prime\prime})^{-2} \\ (U_{D\prime})^{-2} = (U_{D\prime\prime})^{-2}\end{cases}$ *can't happen by their definition unless* $D' = D''$ *and we are done.*

Interestingly the above parameter space has been shown with high significance to posess a causal structure in terms of parameter-space interval identical to the causal structure induced on an interval of spacetime in the usual Minkowski space (see section 6 for numerical analysis).

5. The informational Minkowski-like metric of the dendrogramic space

Having established the existence of spaces with four parameters that uniquely determine a dendrogram, we can now develop an informational metric inspired by Minkowski spacetime. We will describe our model step by step: each parameter point θ in parameter space uniquely defines a dendrogram with n_θ events. This dendrogram is the n level state of an ensemble of observers with same dendrogram. Thus the point θ has a flow-in of observers from different smaller dendrograms with $n-1$ events. The distribution of observers over these smaller dendrograms can be converted to an observers distribution over $\boldsymbol{\theta'}$. where $\boldsymbol{\theta'}$ are parameter points of all dendrograms with $n-1$ events. This is the past observer distribution of θ

Furthermore, the dendrogram at level n, at point θ, exhibits a flow of observers emanating from the θ parameter point. The ensemble of observers, at θ, is distributed to the next level dendrograms with $n-1$ events. This certain manner of distribution of the observers represents the future distribution of the n-level θ point.

Specifically, for a single dendrogram at level n, its future cone at levels n+k (where k ranges from 1 to M→∞) consists of k distributions $\rho_{k,n}(\theta')_{future}$, dependent on the level (or number of events in dendrogram) of the initial θ' point in the parameter space at that level n. Similarly, the past cone of a dendrogram at level n extends to level n-k (where k ranges from 1 to n-2) and exhibits k distributions $\rho_{k,n}(\theta')_{past}$ (see Figure 5).

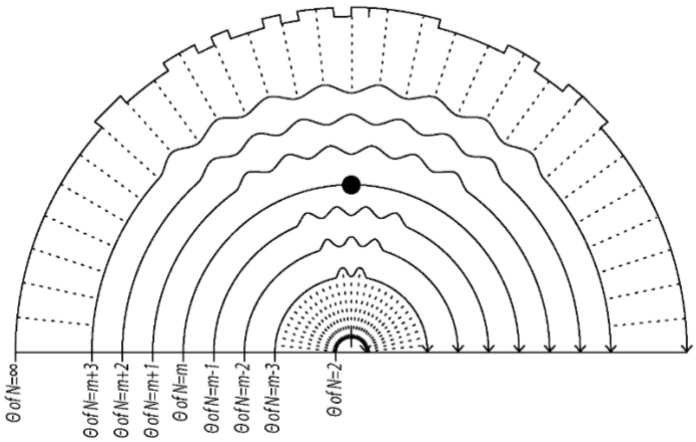

Figure 5: representation of a point in the dendrogramic parameter space and it's accompanied distributions in each of the future and past levels. Half circled distributions are over $\boldsymbol{\theta}$'s possible for each level.

As k approaches infinity, the distributions tend to flatten, meaning that at infinity each observer acquires a unique infinite dendrogram. Therefore, at infinity, the particular point θ' has a distribution of 1/N (where N is the number of observers at θ'), as each observer possesses a unique dendrogram. The subset of all infinite dendrograms belonging to the point θ' defines θ', and vice versa. Consequently, if there exists an intersection between the infinite dendrograms associated with $\theta'1$ and $\theta'2$, it implies that there are observers flowing from one point to the other, establishing a causal connection or indicating timelike separation between the two parameter points. On the other hand, if the intersection is an empty set, it signifies spacelike separation between the two parameters.

We conclude by stressing that a point θ in parameter space is accompanied with all its past distributions flowing into that point and all future distribution flowing out of that point. These distributions and the point θ are defined either by the set of the observers that flow in and out of the θ point or the set of ultimate infinite dendrograms, defining unique observers, and vice versa (figure 5).

These distributions dynamics is manifested from level to level by a "potential"/"force" we call the "Leibnitz potential/force" which forces the observers to become distinct (ultimately at the ontic infinite sub dendrogram). Other wise Leibnitz principle holds where:

Leibniz principle (identity of indiscernibles) states that If, for every property F, object x has F if and only if object y has F, then x is identical to y. in our case it translates to If, for every dendrogram D_∞, observer x has D_∞ if and only if observer y has D_∞, then observer x is identical to observer y.

This is an infect the ontic realization of Leibnitz principle.

To quantify the informational distance between two parameter points accompanied with their distribution, we propose an informational geometric metric:

$$informational\ distance = 2H_f^{\lceil T \rceil} + 2H_p^{\lceil T \rceil} - \left(H_{f'} + H_{p'}\right) - 2\left(\frac{L}{L+1}H_{ratio} + \lceil T \rceil\right) \quad (5)$$

Consider two points $\theta'1$ *and* $\theta'2$ *and* $n1, n2$ *are their level where without loss of generality* $n1 \leq n2$*:*

H_f *=Hellinger distance between* $\rho_{k,n1,\theta'1}(x)_{future\ at\ n2+1}$ *and* $\rho_{k,n2,\theta'2}(x)_{future\ at\ n2+1}$ *(see figure 6), if* $\rho_{k,n1,\theta'1}(x)_{future\ at\ n2+1}$ *and* $\rho_{k,n2,\theta'2}(x)_{future\ at\ n2+1}$ *share parameter points with non zero probability* $0 \leq H_f < 1$ *else* $H_f = 1$

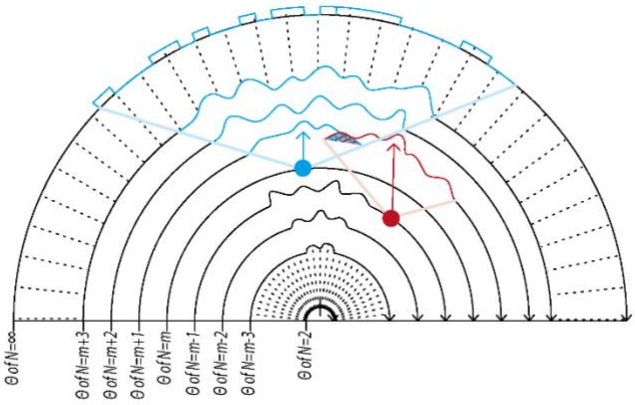

Figure 6: representation of the H_f =*Hellinger distance between* $\rho_{k,n1,\theta'1}(x)_{future\ at\ n2+1}$ *and* $\rho_{k,n2,\theta'2}(x)_{future\ at\ n2+1}$. *Blue distributions over possible* θ*'s of blue point. Red distributions over possible* θ*'s of Red point. Grey area is where blue and red distributions share* θ*'s*

H_p =*Hellinger distance between* $\rho_{k,n1,\theta'1}(x)_{past\ at\ n1-1}$ *and* $\rho_{k,n2,\theta'2}(x)_{past\ at\ n1-1}$ *(see figure 7), if* $\rho_{k,n1,\theta'1}(x)_{past\ at\ n1-1}$ *and* $\rho_{k,n2,\theta'2}(x)_{past\ at\ n1-1}$ *share parameter points with non zero probability* $0 \leq H_f < 1$ *else* $H_f = 1$

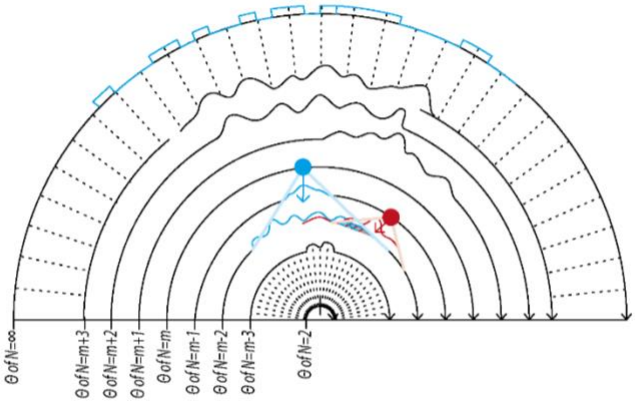

Figure 7: representation of the H_p =*Hellinger distance between* $\rho_{k,n1,\theta'1}(x)_{past\ at\ n1-1}$ *and* $\rho_{k,n2,\theta'2}(x)_{past\ at\ n1-1}$. *Blue distributions over possible* θ*'s of blue point. Red distributions over possible* θ*'s of Red point. Grey area is where blue and red distributions share* θ*'s*

$\rho_{k,\overset{\cdots}{n1},\theta'1}(x)_{\ future\ n1+k1}$ = *lowest k1 value distribution of* $\theta'1$ *that shares parameter points with non zero probability, lowest k2 value with* $\rho_{k,n2,\theta'2}(x)_{future\ n2+k2}$. *Thus:*
$H_{f'}$ =*Hellinger distance between* $\rho_{k,\overset{\cdots}{n1},\theta'1}(x)_{\ future\ n1+k1}$ *and* $\rho_{k,n2,\theta'2}(x)_{future\ n2+k2}$ *(figure 8)*

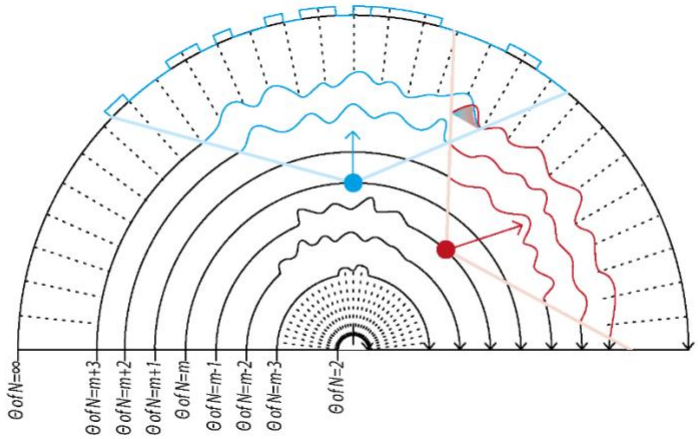

Figure 8: representation of the H_f, =*Hellinger distance between* $\rho_{k,n\dot{1}\dot{1},\theta'1}(x)_{\ future\ n1+k1}$ *and* $\rho_{k,n2,\theta'2}(x)_{future\ n2+k2}$. *Blue distributions over possible* θ*'s of blue point. Red distributions over possible* θ*'s of Red point. Grey area is where blue and red distributions share* θ*'s*

$\rho_{k,n\dot{2}\dot{2},\theta'2}(x)_{\ past\ n2-k2}$ = *lowest k2 value distribution of* $\theta'2$ *that shares parameter points, with non zero probability, with lowest k1 value distribution* $\rho_{k,n1,\theta'1}(x)_{past\ n1-k1}$. *Thus:*
H_p, =*Hellinger distance between* $\rho_{k,n\dot{2}\dot{2},\theta'2}(x)_{\ past\ n2-k2}$ *and* $\rho_{k,n1,\theta'1}(x)_{past\ n1-k1}$ *(figure 9)*

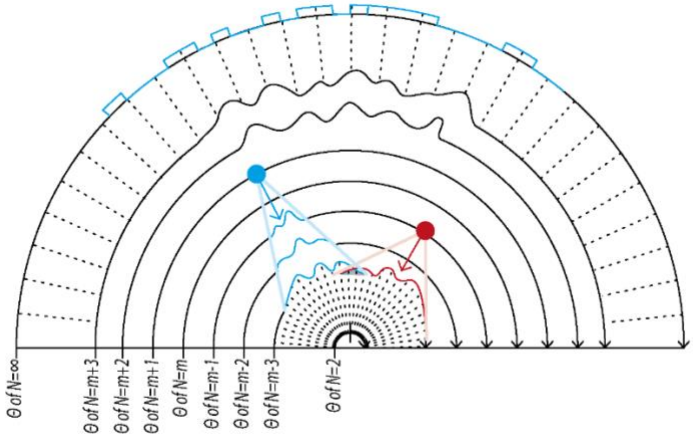

Figure 9: representation of the H_p, =*Hellinger distance between* $\rho_{k,n\dot{2}\dot{2},\theta'2}(x)_{\ past\ n2-k2}$ *and* $\rho_{k,n1,\theta'1}(x)_{past\ n1-k1}$. *Blue distributions over possible* θ*'s of blue point. Red distributions over possible* θ*'s of Red point. Grey area is where blue and red distributions share* θ*'s*

$$L = |n1 - n2|$$

H_{ratio} = *Hellinger distance of two distributions* $p_{pop\ \theta'1}$ *and* $p_{pop\ \theta'2}$
Where $p_{pop\ \theta'1} =$

$$\left[\frac{number\ of\ observers\ at\ point\ \theta'1\ at\ lenvel\ n1}{total\ number\ of\ observers} \quad \frac{number\ of\ observers\ at\ points\ other\ then\ \theta'1\ at\ level\ n1}{total\ number\ of\ observers}\right]$$

$p_{pop\ \theta'1} =$

$$\left[\frac{number\ of\ observers\ at\ point\ \theta'2\ at\ level\ n2}{total\ number\ of\ observers} \quad \frac{number\ of\ observers\ at\ points\ other\ then\ \theta'2\ at\ level\ n2}{total\ number\ of\ observers}\right]$$

$T = p_{\theta'1}(x = \theta'2)$ =*distribution value of* $\rho_{k,n1,\theta'1}(x)_{future\ at\ n2}$ *at* $x=\theta'2$ *see figure 10.*

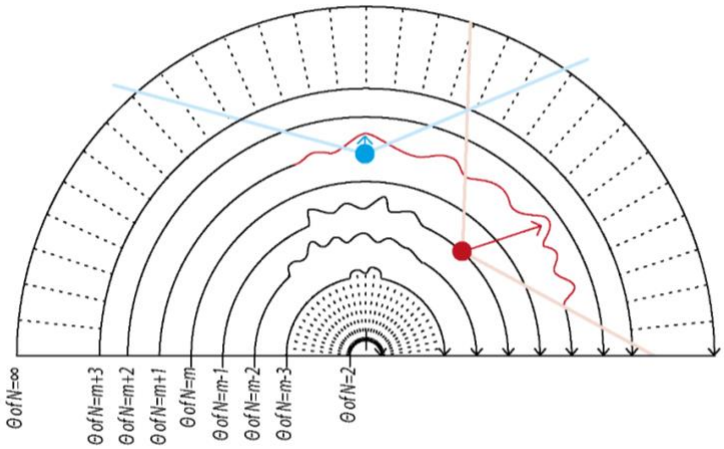

Figure 10: representation of $T = p_{\theta'1}(x = \theta'2)$ =*distribution value of* $\rho_{k,n1,\theta'1}(x)_{future\ at\ n2}$ *at* $x=\theta'2$. *Red distribution has non zero value at the blue point* θ

Now for proving the timelike/spacelike signature:
For time like dendrograms H_f=$H_{f'}$, $H_p = H_{p'}$ and $\lceil T \rceil = 1$. Thus, the metric reduces to :
$informational\ distance = H_f + H_p - 2\left(\frac{L}{L+1}H_{ratio} + \lceil T \rceil\right)$.
$0 \le H_f + H_p < 2$ since they are timelike. On the other hand : $H_{ratio} \le 1$, $\frac{L}{L+1} < 1$
As $\left\lceil p_{\theta'1}\left(x = \theta'2\right)\right\rceil = \lceil T \rceil = 1$ as in timelike dendrograms some fraction of observer flow from one dendrogram to the other.
So the component $2 \le 2\left(\frac{L}{L+1}H_{ratio} + \lceil T \rceil\right)$ resulting in :

$$H_f + H_p - 2\left(\frac{L}{L+1}H_{ratio} + \lceil T \rceil\right) < 0$$

Now for space like, we have in fact two cases lets treat the first one where n1<n2
$H_f = 1, H_p = 1$ thus we reduce the metric to $4 - (H_{f'} + H_{p'}) - 2\left(\frac{L}{L+1}H_{ratio} + \lceil T \rceil\right)$.

$$0 < (H_{f'} + H_{p'}) \le 2 \longrightarrow\ 4 - (H_{f'} + H_{p'}) \ge 2$$

Then for $2\left(\frac{L}{L+1}H_{ratio} + \lceil T \rceil\right)$ we have again $H_{ratio} \le 1$, $\frac{L}{L+1} < 1$ but $\left\lceil p_{\theta'1}\left(x = \theta'2\right)\right\rceil = \lceil T \rceil = 0$ so $2\left(\frac{L}{L+1}H_{ratio} + \lceil T \rceil\right) < 2$

The other case is when $H_f < 1, H_p < 1$ then H_f=$H_{f'}$, $H_p = H_{p'}$ and $\lceil T \rceil = 0$ leading to

$$informational\ distance = 4 - (H_f + H_p) - 2\left(\frac{L}{L+1}H_{ratio} + \lceil T \rceil\right)$$

Again $0 \le H_f + H_p < 2$ thus $4 - (H_{f'} + H_{p'}) \ge 2$ but $2\left(\frac{L}{L+1}H_{ratio} + \lceil T \rceil\right)$ reduces to

$$2\left(\frac{L}{L+1}H_{ratio}\right) < 2$$

Thus: $4-(H_{f'}+H_{p'})-2\left(\frac{L}{L+1}H_{ratio}+\lceil T \rceil\right)>0$

For n1=n2

We have if $H_f=1, H_p=1 \rightarrow\ 4-(H_{f'}+H_{p'})-2\left(\frac{L}{L+1}H_{ratio}+\lceil T \rceil\right)$ since $\lceil T \rceil=0$ and $L=0$ thus $2\left(\frac{L}{L+1}H_{ratio}+\lceil T \rceil\right)$=0 and we have $4-(H_{f'}+H_{p'})\geq 2$

And we are done

If We have if $H_f<1, H_p<1 \rightarrow\ 4-(H_{f'}+H_{p'})-2\left(\frac{L}{L+1}H_{ratio}+\lceil T \rceil\right)$ since $\lceil T \rceil=0$ and $L=0$ where $H_f=H_{f'}$, $H_p=H_{p'}$ we conclude that $2\left(\frac{L}{L+1}H_{ratio}+\lceil T \rceil\right)$=0 and we have $4-(H_{f'}+H_{p'})\geq 2$

And we are done.

6. Establishing dendrogram-parameters coupling via numerical simulation

Although the informational geometric Minkowski-like metric is proved analytically, in practical data analysis applications, we still face the problem of determining which two dendrograms are “time-like” and which are “space-like”. For that purpose we need parameter spaces that follow the usual Minkowski space-time determinant where it must possess the light-cone characteristics. In the context of spacetime intervals spacelike intervals are characterized by $\sum \Delta X^2 > c\Delta t^2$ whereas time-like intervals are characterized by $\sum \Delta X^2 < c\Delta t^2$

The problem of encoding dendrograms using real parameters is mathematically challenging and can require a significant amount of time to find a solution. In the context of DHT- theory, where simulations have provided valuable insights, we propose a method called "numerical experimenting confirmation" to select parameters. Through an extensive numerical simulation, we demonstrate the validity of our real parametrization on the space of dendrograms. While this approach does not provide a mathematical proof of the minkowski-like determinant, the likelihood of encountering dendrograms that do not conform to our parametrization is practically negligible. As a result, we confidently propose the use of this parametrization for the extended space of dendrograms. In this technical section, we present the output and findings of our numerical simulation.

In appendix A1 we outline the numerical procedures for generating different observers with certain n=5,6,7 events encoded in their dendrograms (process 1 and 2). Each initial level n has m number of unique dendrograms (for each of the m unique dendrograms we created 100 different observers).We then investigate which dendrograms, with n+k events, where] k=1,2..6 , each such observer can reach by adding to its n previous events k random events (process 3).In that way we could know for a single observer in its initial “events-level n” what are its possible dendrogram it can transfer to in each of the “events-level n+k”

In each scenario of n+k events, starting from one of the m initial n level dendrogram, we examined the set of possible unique dendrograms that could be created. This analysis allowed us to determine the distribution of these unique n+k events dendrograms that arise from any of the m's unique initial dendrogram as shown in figure S1 in supplementary material for n=6.

Interestingly, all m dendrograms with n=6 could be transformed to all possible dendrograms at n+k levels where k has the value of 3-4. However, for the m dendrograms with n=7, this encompassing did not occurr. This implies that some of the m initial dendrograms with n=6,7 had both "space like" and "time like" as their future evolving dendrograms (figure S2 A1-A2; supplementary material).

These results raise the question of whether we can assign Minkowski-like signatures (determinant) to these dendrograms parameter spaces. We require these spaces to posess interval values opposite in sign dependent on whether two dendrograms can or cannot evolve to each other.

Interestingly, the absolute difference between some of the 60 parameter values (described in section 3) of an initial dendrogram (one of the m possible) and its corresponding dendrograms it evolved to, at some level n+k, showed significant difference compared to the absolute difference between the parameter values an initial dendrogram (one of the m possible) and its corresponding dendrograms **it did not evolve to**, at some level n+k.

After performing 5000 iterations of random selection for z, z1, z2, z3, and z4, we identified 23 out of the 60 parameters that exhibited statistical significance ($p < 0.05$ in t-test) in at least 60% of the occurrences where "timelike" and "spacelike" dendrograms both existed for an initial specific m dendrogram. Furthermore, these parameters showed significance in at least 70% of the random selections of z, z1, z2, z3, and z4 introduced in section 3 (an example is shown in figure S2 B.1-B.2).

With those 23 parameters we examined all possible combinations such that:

$$INTERVAL_i = (\theta'_{i\ initial\ dendrogram} - \theta'_{i\ n+k\ level\ dendrogram})^2 \quad for\ i = 1,2,3$$

Where we define *n= initial dendrogram level/ number of events*
n+k=level of transmitted/not transmitted dendrograms, k=1,2,3,4,5,6.

$$INTERVAL_4 = (\sqrt{n}\theta'_{i\ initial\ dendrogram} - (\sqrt{n+k})\theta'_{i\ n+k\ level\ dendrogram})^2 \quad for\ i = 4$$

Such that the following equation :

$$INterval = INTERVAL_1 + INTERVAL_2 + INTERVAL_3 - s2 * INTERVAL_4 \tag{6}$$

Will fulfill the condition that $INterval$ values for spacelike and timelike dendrograms have opposite signs

We conducted 5000 iterations, exploring various combinations of constants (z, z1, z2, z3, z4, and s2), to identify parameter sets consistently demonstrating opposite sign intervals between timelike and spacelike dendrograms. This analysis encompassed all initial m dendrograms (limited to n=6) and their corresponding spacelike/timelike dendrograms at n+k levels (k=1, 2, ..., 6).

Remarkably, our analysis revealed the existence of parameter spaces with two distinct causality structures: one characterized by a "negative spacelike signature" and the other by a "positive spacelike signature."

In the case of the "negative spacelike signature," we observed that the interval between two spacelike dendrograms was consistently negative (for n=6 and all n+k, k=1,2..6 levels). This negative signature held true across all intervals computed from the parameters of the 9 initial n=6 level dendrograms and their corresponding n+k spacelike dendrograms (where k ranged from 1 to 6). Notably, the timelike dendrograms derived from each of the n=6 initial dendrograms consistently exhibited positive values for their respective time-like parameter intervals. Importantly, this reversed causality structure was consistently observed across all 9 initial dendrograms and their unique sets of n+k dendrograms (totaling 21, 51, 127, 127, 834, and 2400 such unique dendrograms for k=1, 2, ..., 6, respectively).

This observation contradicts the ordinary causal structure of the real Minkowski metric in special relativity and its resulting characteristic light-cone , where information cannot be transmitted between two spacelike separated events for the trivial cause that the sum of the space coordinates' intervals is greater than the distance light can travel within the given time interval.

Conversely, the "positive spacelike signature" aligns with the characteristics of the Minkowski metric. this positive "space like signature" remained consistent for all intervals computed from the parameters of the 9 initial n=6 level dendrograms and their corresponding n+k spacelike dendrograms (with k ranging from 1 to 6). this Minkowski-like causality structure persisted across all 9 initial dendrograms and their unique sets of n+k dendrograms (totaling 21, 51, 127, 127, 834, and 2400 such dendrograms for k=1, 2, ..., 6, respectively).

In our random numerical analysis, we observed a higher occurrence of parameter spaces with a "positive spacelike signature" compared to those with a "negative spacelike signature." Remarkably, each of these two distinct parameter spaces maintained consistency and demonstrated opposite sign intervals between timelike and spacelike dendrograms across all initial n=6 dendrograms and their corresponding n+k level dendrograms.Figure S3 illustrates the overall rather peculiar and counter-intuitive causality, where timelike intervals have positive values and spacelike intervals have negative values. Figure S4 on the other hand illustrates the elignment of the “positive spacelike signature” with the regular Minkowski causal spacelike structure.

Out of the 5000 randomly generated combinations of constants (z, z1, z2, z3, z4, and s2), our analysis identified 260 distinct combinations that demonstrated consistency across all n+k levels for the initial set of 9 dendrograms with n=6. This consistency was defined by the inverse sign between the computed $INterval$ values, as defined in equation 6, for the timelike dendrograms and their corresponding spacelike dendrograms.

In total, we discovered a total of 3117 different combinations of constants (z, z1, z2, z3, z4, s2) and parameters (θ'_1, θ'_2, θ'_3, θ'_4) that exhibited this remarkable consistency. Among these combinations, 797 displayed a "negative spacelike signature," while 2320 exhibited a "positive spacelike signature" (as depicted in Figure 11).

We then verified the consistency of the found sets of these 3117 parameters and constants in the same way for the initial dendrograms of n=5 and n=7.

We observed that when preparing the dendrogram parameters according to the above described method, only specific combinations of θ'_1 , θ'_2 , θ'_3 and θ'_4 can uniquely describe a dendrogram. Such uniqueness is achieved when one of the parameters (θ'_1 , θ'_2 or θ'_3) is either V_D or U_D, and another parameter is a product, sum, or division of the two. Alternatively, when one of the parameters is R_D or r_D, and another parameter is a product, sum, or division of the two.

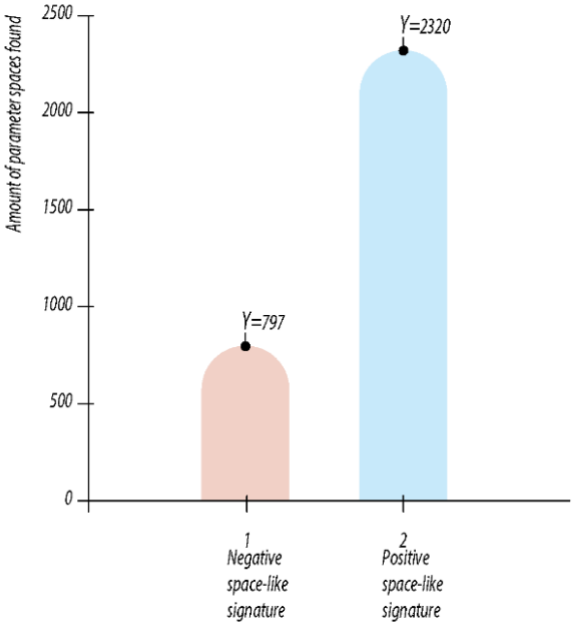

Figure 11: number of "negative spacelike signature and positive spacelike signature parameter spaces found in our simulations

Interestingly, we discovered that all 797 combinations with a "negative spacelike signature" were unable to uniquely define the dendrogram space. This suggests that in order for a coordinate/parameter space to uniquely define events (or dendrograms in our case), as is the case in ordinary spacetime, it must possess the Minkowski light-cone

characteristics and vice versa. In these cases with "negative spacelike signature," where this condition was reversed, we lost the uniqueness definition of dendrograms.

Out of the total 2320 consistent parameters that exhibited a "positive spacelike signature," only 310 combinations were found to uniquely define the dendrogram space (refer to Figure 12).

To further investigate this conjecture, we examined a mixture of 760*137 parameter combinations that possessed either a "negative spacelike signature" or a "positive spacelike signature" in n=6 while still being able to uniquely define the dendrogram space.

As expected, all the parameters with a "negative spacelike signature" could not exhibit consistent opposite signs for all m unique initial dendrograms with n=5,7 and their corresponding n+k level spacelike/timelike dendrograms where k=1,2..6. Consequently, these parameters failed to maintain the causal structure of the “reversed” non-trivial light-cone for all n’s.

Thus in cases of parameters exhibiting consistent "negative spacelike signature" with “reversed” causal structure and non-trivial light-cone they fail to uniquely define the dendrogram space. while in cases that do possess the ability to uniquely define the dendrograms space the "negative spacelike signature" loose consistency of this reversed causal structure.

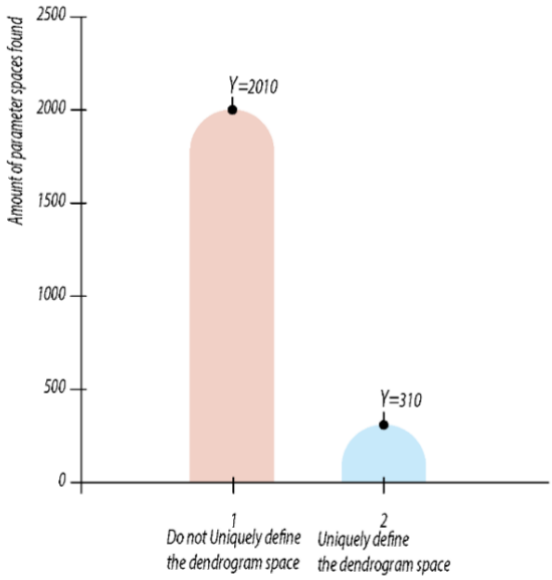

Figure 12: number of positive spacelike signature that uniquely define the dendrogram space vs positive spacelike signature that did not uniquely define the dendrogram space found in our simulations.

On the other hand, some of the parameter spaces (49 of them) with a "positive spacelike signature" exhibited the necessary consistency of the causal structure of the light cone, in all tests conducted for n=5, 6, and 7 (as described earlier). This outcome confirmed

that the only possible causal structure must resemble the ordinary Minkowski metric light cone.

In order to validate the applicability of the 310 combinations of $\theta'_1, \theta'_2, \theta'_3$ *and* θ'_4 that were both consistent and could uniquely define the dendrogram space we conducted the following test: 20000 times we randomly generated a dendrogram with a random size smaller than 100 events and its corresponding timelike dendrogram, which was obtained by adding random k events to the initial dendrogram. The value of k satisfied the condition; *number of events in initial dendrogram<k<2*number of events in initial dendrogram*
Among the 20,000 tests conducted on "positive space-like signature spaces" none of the cases yielded positive values, thereby illustrating the consistency of the time-like negative signature. This finding is exemplified in Figure 13.

One of the parameter spaces that showed consistency in all m dendrograms for all n=5,6,7 and k=1,2…6 proved to uniquely define the dendrogram space already in section 3.

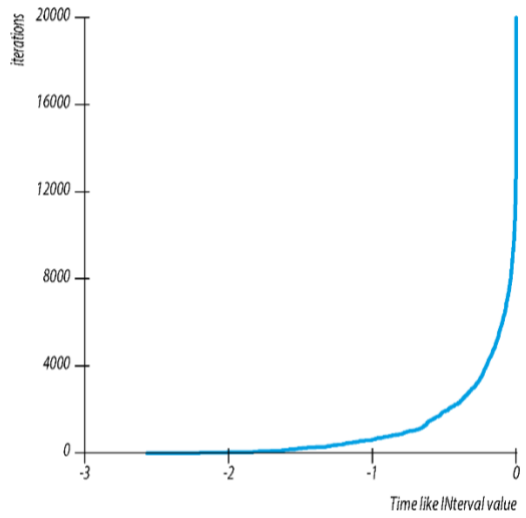

Figure 13: Illustration of the consistency of one time-like negative signature of one parameter space found in our simulations. This parameter space uniquely defined the dendrogramic space

Now for the consequence of our numerical analysis. We propose that

$$p_{\theta'}(X) = \frac{1}{(2\pi a^2)^2} \exp\left(-\frac{(t - i(s2)\theta'_4)^2 + (x - \theta'_1)^2 + (y - \theta'_2)^2 + (z - \theta'_3)^2}{2a^2}\right)$$

Where X is a vector of [t,x,y,z] and s2 is our equivalent of c=speed of light and is defined above in equation 6.
this distribution is normalized: meaning $\int d^4x\, p_{\theta'}(X) = 1$
and leads to

the following fisher information matrix $g_{\mu\nu} = \begin{pmatrix} -s2 & 0 & 0 & 0 \\ 0 & 1 & 0 & 0 \\ 0 & 0 & 1 & 0 \\ 0 & 0 & 0 & 1 \end{pmatrix}$

After rescaling by a^2 [44].
Furthermore, we define *n=number of events in dendrogram 1, n'=number of events in dendrogram 2,*
N=|n-n'| and we define the simultaneity matrix or operator for the positive signature space like combinations

$$\widehat{sym}_+ = \begin{pmatrix} \lceil \frac{N}{N+1} \rceil & 0 & 0 & 0 \\ 0 & 1 & 0 & 0 \\ 0 & 0 & 1 & 0 \\ 0 & 0 & 0 & 1 \end{pmatrix}$$

$$dist(dendrogram1, dendrogram2) = \widehat{(sym}_+)_{\mu\nu} g_{\mu\nu} d\theta'_\mu d\theta'_\nu$$

One benefit of this construction is the transformation of the discrete parameter space into a continuous one. Thus, every dendrogram is defined by its non-hermitian distribution $p_{\theta'}(X)$ defined above (ref) and we operate on a smooth Riemann 4d parameter space. In that way we can also find the null like parameters for a given dendrogram (although they will (probably) not represent a dendrogram)

6. Concluding remarks

Exploring of the treelike geometry opens a new direction in modelling of the event universe endowed with hierarchic relational structure. At the epistemic level, experimental data collected by an observer is represented with the aid of clustering algorithm by a dendrogram – a finite tree. Collection of new data restructures observer's dendrogram. Such dynamical restructuring is nonlocal w.r.t. the hierarchic relation between events: appearance of a new event restructures whole dendrogram. We emphasize that this is relational nonlocality, w.r.t. p-adic ultrametric on a tree, not nonlocality in the physical spacetime. As we know relational mechanics and event universe play the important role in the modern development of quantum foundations [35,36,38,45–49]. Our approach, DHT [1–8], gives the new mathematical and physical insights to this area of research. Of course, it is important to connect relational event physical models with conventional models based on the real space-time endowed with Minkowski's causal structure. In the present paper we proceed in this direction. We start with introduction of the causal structure on the dendrogramic configuration space. This causality is statistical and reflects dendrogramic dynamics for ensembles of observers. This is the novel approach to causality. Then we encode dendrograms by real parameters. This gives the possibility to determine the four-dimensional real space-time and information geometry on it matching the statistical observers' causality. The possibility to use dimension four for

representation of dendrograms of any size is surprising and at the same time supporting for dendrogramic modeling of causality and its coupling with causality in Minkowski spacetime.

We emphasize again, the real parameter spaces revealed through our numerical analysis, while associated with a collective of observers, primarily encapsulate the entirely subjective and observer-dependent knowledge of an individual observer concerning the universe. Consequently, these spaces inherently exhibit subjectivity.

Via this construction, transformations of special relativity can be realized on the dendrogramic configuration space. This is the topic for the further development of DHT. Finally, we remark once again that DHT finds applications outside of physics, in modelling of information processing by the brain and medical diagnostics of the brain disorders. The method developed in the present paper gives the possibility to invent a kind of Minkowski causal structure on the mental space. In future studies, we shall employ this structure for medical diagnostics.

References:

[1] Shor O, Benninger F and Khrennikov A 2021 Representation of the universe as a dendrogramic hologram endowed with relational interpretation *Entropy* **23**

[2] Shor O, Benninger F and Khrennikov A 2021 Dendrogramic representation of data: Chsh violation vs. nonergodicity *Entropy* **23**

[3] Shor O, Benninger F and Khrennikov A 2022 Towards Unification of General Relativity and Quantum Theory: Dendrogram Representation of the Event-Universe *Entropy* **24**

[4] Shor O, Benninger F and Khrennikov A 2022 Dendrographic Hologram Theory: Predictability of Relational Dynamics of the Event Universe and the Emergence of Time Arrow *Symmetry (Basel)* **14**

[5] Shor O, Benninger F and Khrennikov A 2022 Emergent quantum mechanics of the event-universe, quantization of events via Denrographic Hologram Theory *arXiv preprint arXiv:2208.01931*

[6] Shor O, Benninger F and Khrennikov A *Rao-Fisher information geometry and dynamics of the event-universe views distributions*

[7] Shor O, Glik A, Yaniv-Rosenfeld A, Valevski A, Weizman A, Khrennikov A and Benninger F 2021 EEG p-adic quantum potential accurately identifies depression, schizophrenia and cognitive decline *PLoS One* **16** e0255529-

[8] Shor O, Yaniv-Rosenfeld A, Valevski A, Weizman A, Khrennikov A and Benninger F 2023 EEG-based spatio-temporal relation signatures for the diagnosis of depression and schizophrenia *Sci Rep* **13** 776

[9] Leibniz G W 1989 *The Monadology: 1714* (Springer)

[10] Schikhof W H 2007 *Ultrametric Calculus: An Introduction to P-Adic Analysis* (Cambridge University Press)

[11] Vladimirov, V.S., Volovich, I.V., Zelenov E I 1994 *P-adic Analysis and Mathematical Physics* (World Scientific, Singapore)

[12] Volovich I V p-adic string *Class. Quantum Gravity* **4** 83–87

[13] Aref'eva, I. Ya., Dragovich, B., Frampton, P. H., Volovich I V. The wave function of the Universe andp-adic gravity *Int. J. Mod. Phys* **A6** 4341–4358

[14] Freund P G O and Witten E 1987 Adelic string amplitudes *Physics Letters B* **199** 191–4

[15] Parisi G 1988 On p-adic functional integrals *Mod Phys Lett A* **3** 639–43
[16] Volovich I V. 2010 Number theory as the ultimate physical theory *P-Adic Numbers, Ultrametric Analysis, and Applications* **2** 77–87
[17] Dragovich B, Khrennikov A Yu, Kozyrev S V, Volovich I V and Zelenov E I 2017 p-Adic mathematical physics: the first 30 years *p-Adic Numbers, Ultrametric Analysis and Applications* **9** 87–121
[18] Chen L, Liu X and Hung L-Y 2021 Emergent Einstein equation in p-adic conformal field theory tensor networks *Phys Rev Lett* **127** 221602
[19] Hung L-Y, Li W and Melby-Thompson C M 2019 p-adic CFT is a holographic tensor network *Journal of High Energy Physics* **2019** 1–39
[20] Gubser S S, Heydeman M, Jepsen C, Marcolli M, Parikh S, Saberi I, Stoica B and Trundy B 2017 Edge length dynamics on graphs with applications to p-adic AdS/CFT *Journal of High Energy Physics* **2017** 1–35
[21] Heydeman M, Marcolli M, Saberi I and Stoica B 2016 Tensor networks, $ p $-adic fields, and algebraic curves: arithmetic and the AdS $ _3 $/CFT $ _2 $ correspondence *arXiv preprint arXiv:1605.07639*
[22] Gubser S S, Knaute J, Parikh S, Samberg A and Witaszczyk P 2017 p-adic AdS/CFT *Commun Math Phys* **352** 1019–59
[23] G Parisi 1980 A sequence of approximated solutions to the S-K model for spin glasses *J Phys A Math Gen* **13** L115
[24] G Parisi 1980 The order parameter for spin glasses: a function on the interval 0-1 *J Phys A Math Gen* **13** 1101
[25] Parisi G and Sourlas N 2000 P-adic numbers and replica symmetry breaking *The European Physical Journal B - Condensed Matter and Complex Systems* **14** 535–42
[26] Khrennikov A Yu and Kozyrev S V 2006 Replica symmetry breaking related to a general ultrametric space I: Replica matrices and functionals *Physica A: Statistical Mechanics and its Applications* **359** 222–40
[27] Parisi G and Sourlas N 2000 P-adic numbers and replica symmetry breaking *The European Physical Journal B - Condensed Matter and Complex Systems* **14** 535–42
[28] Barbour J 2012 Shape Dynamics. An Introduction *Quantum Field Theory and Gravity* 257–97
[29] Gryb S 2012 Shape dynamics and Mach's principles: Gravity from conformal geometrodynamics
[30] Brans C and Dicke R H 1961 Mach's principle and a relativistic theory of gravitation *Physical review* **124** 925
[31] Rovelli C 2004 *Quantum Gravity* (Cambridge University Press)
[32] John C Baez 1998 Spin foam models *Class Quantum Gravity* **15** 1827
[33] Dowker F 2013 Introduction to causal sets and their phenomenology *Gen Relativ Gravit* **45** 1651–67
[34] Rovelli C 1996 Relational quantum mechanics *International Journal of Theoretical Physics* **35** 1637–78
[35] Smolin L 2016 Quantum Mechanics and the Principle of Maximal Variety *Found Phys* **46** 736–58
[36] Smolin L 2018 The Dynamics of Difference *Found Phys* **48** 121–34
[37] Barbour J and Smolin L 1992 Extremal variety as the foundation of a cosmological quantum theory *arXiv preprint hep-th/9203041*
[38] Cortês M and Smolin L 2014 The universe as a process of unique events *Physical Review D - Particles, Fields, Gravitation and Cosmology* **90** 1–30
[39] Vanchurin V 2020 The World as a Neural Network *Entropy* **22**

[40] Katsnelson M I and Vanchurin V 2021 Emergent Quantumness in Neural Networks *Found Phys* **51** 94
[41] Zúñiga-Galindo W A 2023 p-adic statistical field theory and deep belief networks *Physica A: Statistical Mechanics and its Applications* **612** 128492
[42] Zúñiga-Galindo W A, He C and Zambrano-Luna B A 2023 p-Adic statistical field theory and convolutional deep Boltzmann machines *Progress of Theoretical and Experimental Physics* **2023** 063A01
[43] Vanchurin V 2022 Towards a Theory of Quantum Gravity from Neural Networks *Entropy* **24**
[44] Calmet J and Calmet X 2004 Metric on a statistical space-time *arXiv preprint math-ph/0403043*
[45] Rovelli C 1996 Relational quantum mechanics *International Journal of Theoretical Physics* **35** 1637–78
[46] Rovelli C, Segre E and Carnell S 2018 *The Order of Time* (Penguin Books Limited)
[47] Smolin L 2019 Einstein's Unfinished Revolution: The Search for What Lies Beyond the Quantum.
[48] Barbour J and Smolin L 1992 Extremal variety as the foundation of a cosmological quantum theory 1–35
[49] Barbour J, Koslowski T and Mercati F 2014 Identification of a Gravitational Arrow of Time *Phys Rev Lett* **113** 181101

Appendix

A1. Dendrogram representation of events-preliminaries

To achieve our objectives, we employ the following procedure to generate a relational structure e.g. a dendrogram where each branch has a 2-adic expansion.

In our approach, we depict events (referred to as Bohr's phenomena) as branches within a dendrogram, which is essentially a finite tree. Figure 1 provides an illustration that describes the construction of a dendrogramic tree from data. These finite trees serve as an observer's epistemic representation of reality and are constructed as follows:

1. Data collection: Measurements are performed to gather the necessary data.
2. Hierarchical clustering algorithm: A hierarchical clustering algorithm is applied, utilizing a chosen distance metric and a specific clustering (linkage function) algorithm.
3. Agglomerative hierarchical cluster tree: Using the selected distance metric and clustering algorithm, an agglomerative hierarchical cluster tree is constructed. Each event, with its unique branch, can be represented by a binary string or a p-adic expansion of yes/no questions.
4. Dendrogram representation: The set of branches in the tree (or the strings that fully describe them) forms the dendrogram. Each branch, corresponding to a measured event, extends from the root to a leaf (referred to as an edge).
5. Relation between events: A longer common path from root to leaf of two branches signifies a closer relation between the corresponding events, based on the chosen distance metric and clustering algorithm.

To represent the dendrogram, we utilize a series of p-adic numbers, with each number encoding the relationship of a single event to the remaining events acquired by the observers. It's important to note that a dendrogram can only be constructed when the number of events is greater or equal 2, as it relies on the relational structure among events. Initially, all N observers have a trivial dendrogram with two branches.

Within the context of an infinite number of events, the ontic description of the event-universe is portrayed as an infinite tree. One class of such trees is p-adic trees, which are homogeneous trees with p > 1 edges branching from each vertex. These trees possess an algebraic structure and a topology consistent with this structure. The p-adic topology is governed by the p-adic ultrametric, satisfying the strong triangle inequality. The p-adic distance between two branches of the tree is determined by their common root, where a longer common root signifies a shorter distance. As branches represent measurements outcomes of events, the space of events, whether finite or infinite, is equipped with a p-adic ultrametric. Therefore, dendrograms encodes hierarchic relations between measurements of events based on p-adic distances, rather than space-time localization of events. This common root distance determines the level of similarity between the measured events. The geometry of this field exhibits peculiar properties, such as all triangles being isosceles, which arise from the strong triangle inequality. Moreover upon defininig “open” and “closed” balls as

$$B_{-}(R;a) = \{x : r_p(a,x) < R\}, B(R;a) = \{x : r_p(a,x) \leq R\}$$

Where $r_p(a,x) = |a-x|_p$ is the p-adic distance between the points a and x.

each dendrogram edge can be represented by a 2-adic number:
$edge_i = \sum_{j=0}^{k} a_j \times 2^j$, where $a_j = 0,1$.

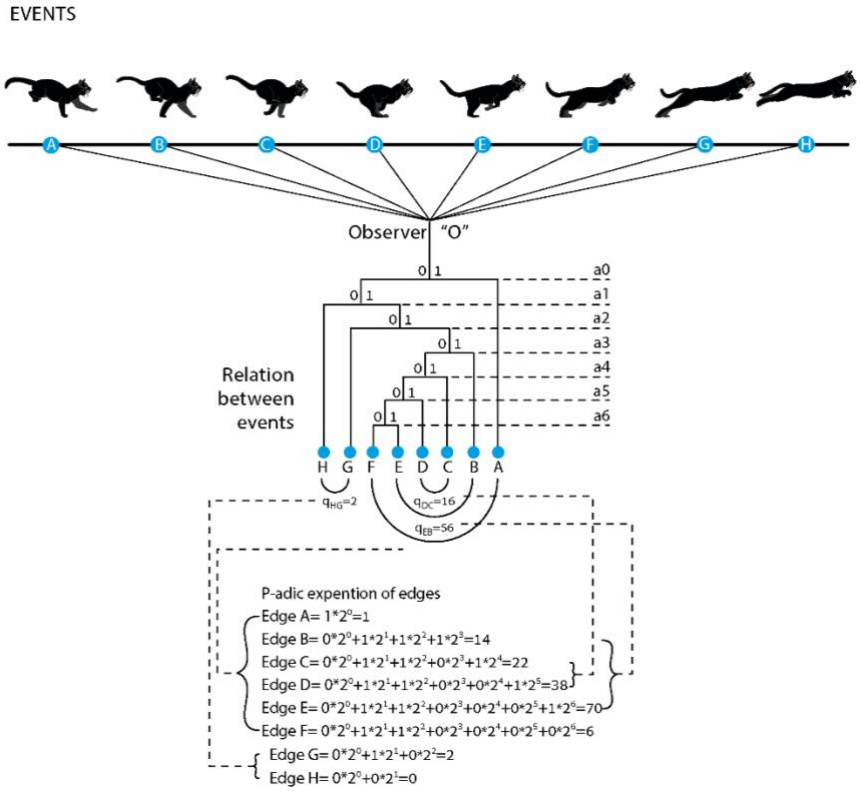

Figure 1.
Relational observation of events. Observer O discriminates events A–H and constructs an object, a dendrogram, which describes the relations between these events. (**B**) Each edge of the dendrogram is a binary string of 0s and 1s which can be represented as a finite p-adic expansion. Each edge summation of its finite p-adic expansion results in a natural number. Subtracting between two edges' finite p-adic expansion results in "potential gap"—qij.

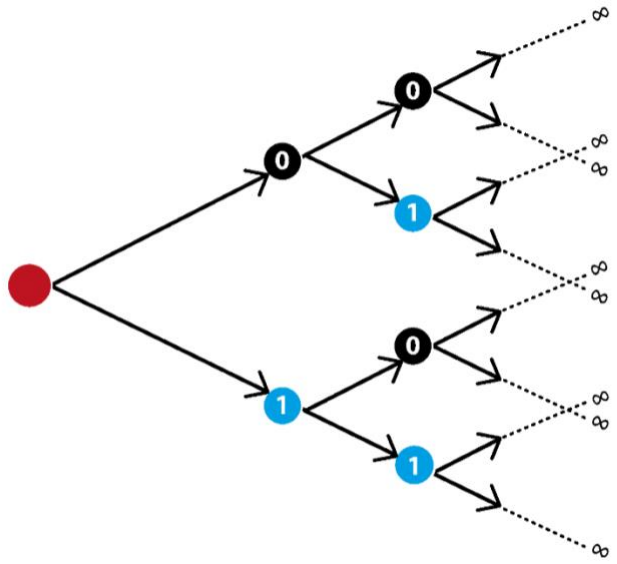

Figure 2. The 2-adic tree

A2. Simulations of "observers" and the possible dendrograms they can reach

process 1 was to determine how many different, unique, dendrograms are possible in some "number of events-level n".

We followed these sub-steps : Here are the sub-steps of the given process:

1. Generate 100,000 vectors of n values (representing events) for each n = 5, 6, and 7 by Randomly selecting n values from the interval [0, 1] for each vector.
2. Compute pairwise Euclidean distances between elements in each vector.
3. Construct agglomerative hierarchical cluster trees using the "single" linkage method for each vector.
4. Identify distinct dendrogram structures for each "number of events-level n".
5. Count the number of different dendrogram structures obtained for each n.

For n=5, we found m=4 different dendrogram structures. For n=6, we obtained m=9 different dendrogram structures, and for n=7, we discovered m=21 different dendrogram structures.

process 2 we produced 100 "observers" for each of the m=4,9,21 unique and different dendrograms each in its corresponding n=5,6,7 event level.

1. randomly select n numbers from the interval [0, 1]
2. construct a dendrogram D out of the n numbers (as in steps 3 and 4 of process 1)
3. identify to which of the m different dendrograms D equals to.
4. the n random numbers defines $Observer_{ij}$ i=1,2..100 j=1,2..m

4.repeat until i=100 for all j

Thus although each of the 100 "observers" collected different n events/numbers their relational observed universe is the same.

Process 3 producing all possible dendrograms an "observer" can evolve to by edding k=1,2..6 events.

1.for each "observer" we add k random numbers (k=1-6) t times (t=4000*(1+k/2) for n=5,6. t=6000*(2+k/2) for n=7)

2. construct a dendrogram D out of the n(constant numbers of the observer) and k random numbers.

Overall, at the end, for all 100 observers we produced for all k=1,2..6 we produced 4*1600000, 9*1600000 and 21*3000000 non unique dendrograms for n=5,6,7 respectively

Supplementary material

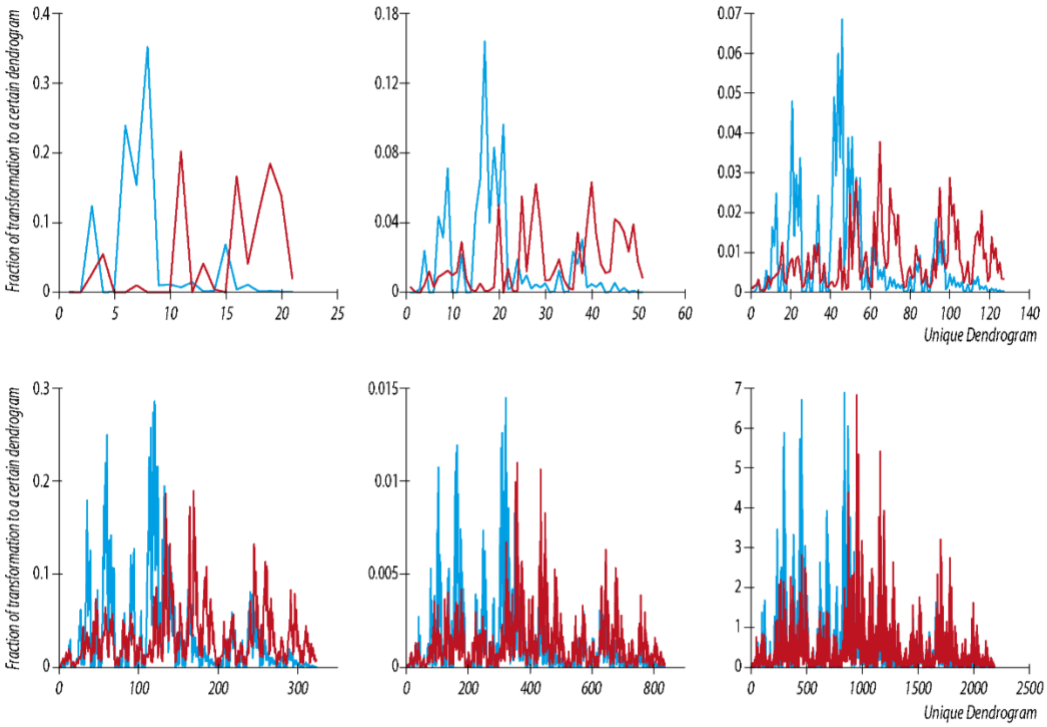

Figure S1: Distribution of Dendrograms at n+k Level for Two Different Initial Dendrograms with 6 Events. This figure illustrates the evolutionary process of two distinct initial dendrograms, namely Dendrogram A and Dendrogram B, each consisting of 6 events. The diagram showcases the distribution of dendrograms that emanate from each initial dendrogram at various n+k levels (k = 1, 2, 3, 4, 5, and 6). At each level, the initial dendrograms undergo transformation and branching, leading to the emergence of unique configurations represented by subsequent dendrogram structures. The visualization offers insights into the dynamic nature of dendrogram evolution as they progress through different levels.

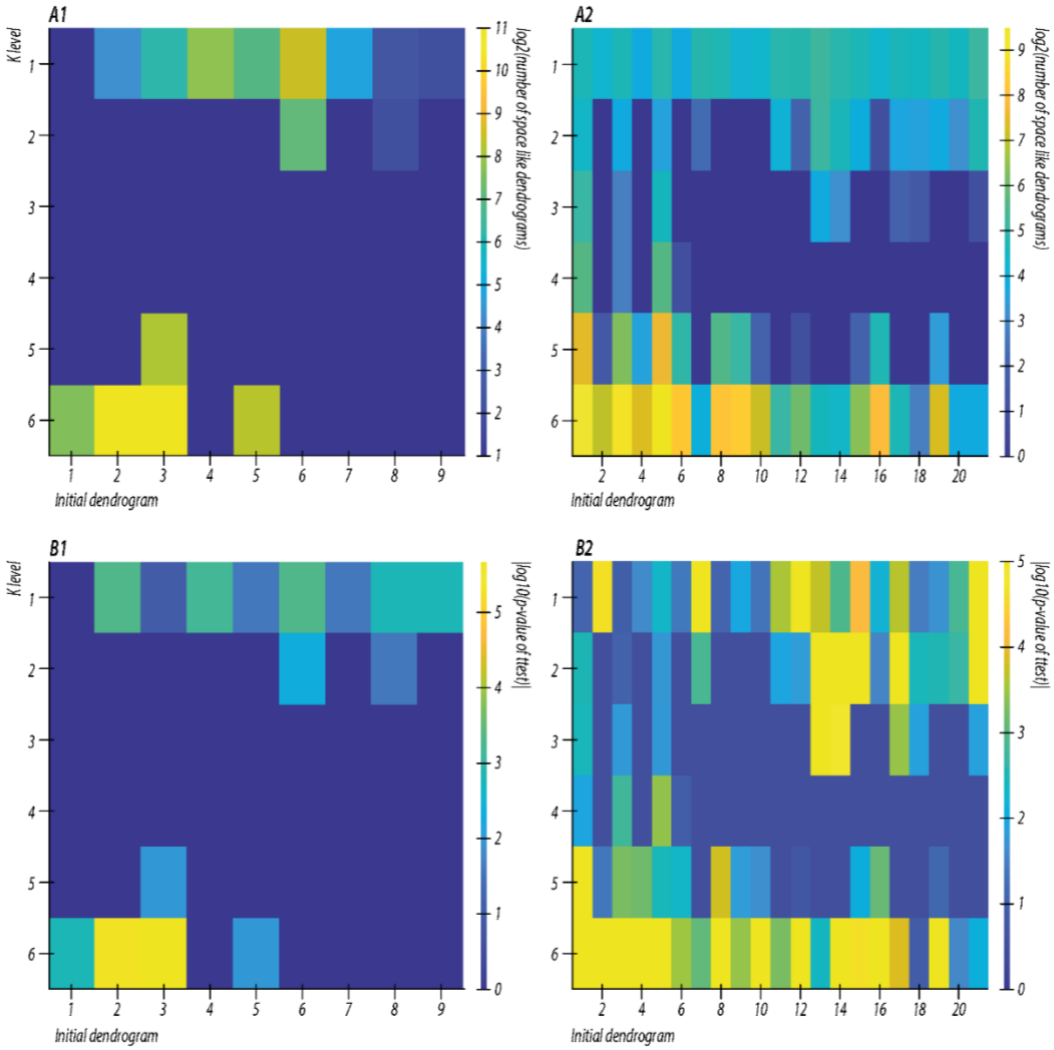

Figure S2:A1 Number of Spacelike Dendrograms for Each k (Initial Level n=6) This subfigure depicts the count of spacelike dendrograms at each k level for various initial dendrograms, all having an initial level of n=6. Each k level demonstrates a distinct number of unique spacelike dendrograms, specifically 21, 51, 127, 323, 835, and 2188, representing different configurations of dendrogram structures. **A2 Number of Spacelike Dendrograms for Each k (Initial Level n=7)** This subfigure displays the count of spacelike dendrograms at each k level for different initial dendrograms, with a shared initial level of n=7. At each k level, there are 51, 127, 323, 835, 2188, and 5798 unique spacelike dendrograms, reflecting diverse configurations of dendrogram structures. **B1 Mean Significance of Intervals in Selected Parameters of Spacelike vs. Timelike Dendrograms (Initial Level n=6)** This subfigure presents the average significance values of intervals within selected parameters for spacelike and timelike dendrograms at each k level, considering various initial dendrograms with an initial level of n=6. The comparison between spacelike and timelike dendrograms allows for an assessment of the significance variations across different intervals in the selected parameters.**B2 Mean Significance of Intervals in Selected Parameters of Spacelike vs. Timelike Dendrograms (Initial Level n=7)** This subfigure exhibits the average significance values of intervals within selected parameters for spacelike and timelike dendrograms at each k level, considering different initial dendrograms with an initial level of n=7. The comparison between spacelike and timelike dendrograms enables an examination of the significance variations across different intervals in the selected parameters.

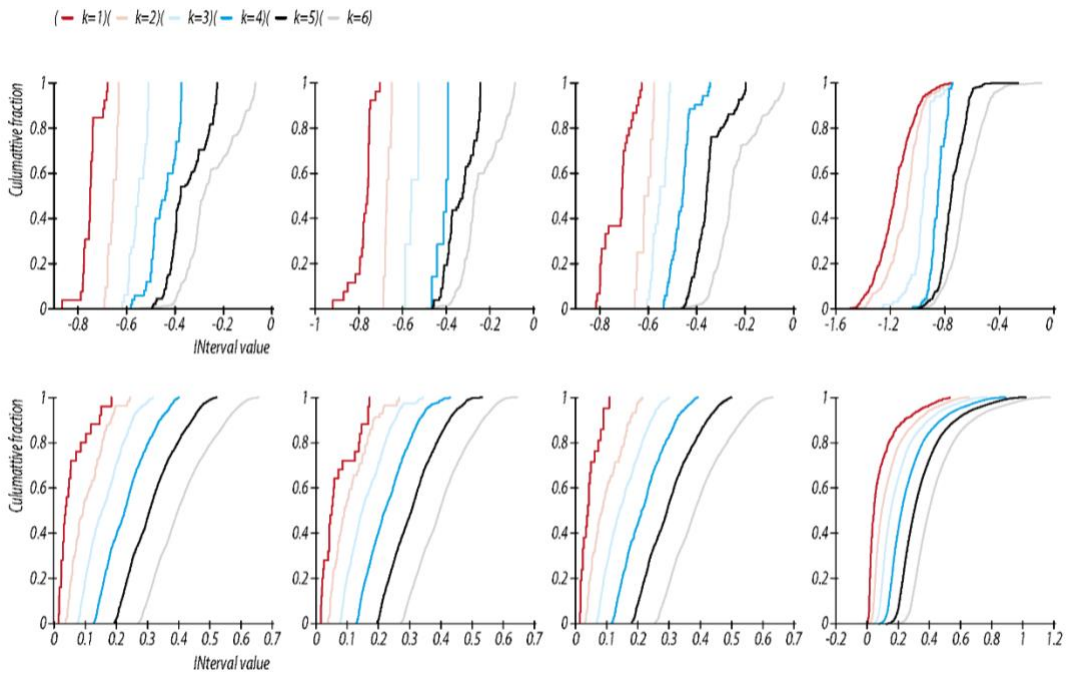

Figure S3: Time-Like and Spacelike Dendrogram Interval Values for the Negative Spacelike Signature Parameter Space

This figure explores the interval values for time-like and spacelike dendrograms in the context of the negative spacelike signature parameter space. The figure is divided into several panels, each representing different aspects of the analysis.**Top row first 3 panels from the left: Cumulative Distribution Functions (cdfs) of Interval Values for Spacelike Dendrograms** depict the cumulative distribution functions (cdfs) of INterval values for spacelike dendrograms, focusing on three specific initial dendrograms at the initial level n=6 and varying k values (k=1, 2, ..., 6). Each panel showcases the distribution of interval values for spacelike dendrograms resulting from the transformation and branching processes. **Top row panel on the right: Cumulative Distribution Function (cdfs) of Interval Values for All Spacelike Dendrograms** presents the cumulative distribution function (cdfs) of INterval values for spacelike dendrograms, encompassing all initial dendrograms at the initial level n=6 and for each k value (k=1, 2, ..., 6). The visualization offers an overall perspective of the interval value distributions across all spacelike dendrograms. **Bottom row first 3 panels from the left: Cumulative Distribution Functions (cdfs) of Interval Values for Time-Like Dendrograms** illustrate the cumulative distribution functions (cdfs) of INterval values for time-like dendrograms, focusing on three specific initial dendrograms at the initial level n=6 and varying k values (k=1, 2, ..., 6). Each panel provides insights into the distribution of interval values for time-like dendrograms resulting from the transformation and branching processes. **Bottom rowrightpanel: Cumulative Distribution Function (cdfs) of Interval Values for All Time-Like Dendrograms** displays the cumulative distribution function (cdfs) of INterval values for time-like dendrograms, encompassing all initial dendrograms at the initial level n=6 and for each k value (k=1, 2, ..., 6). The visualization presents an overall perspective of the INterval value distributions across all time-like dendrograms.

.

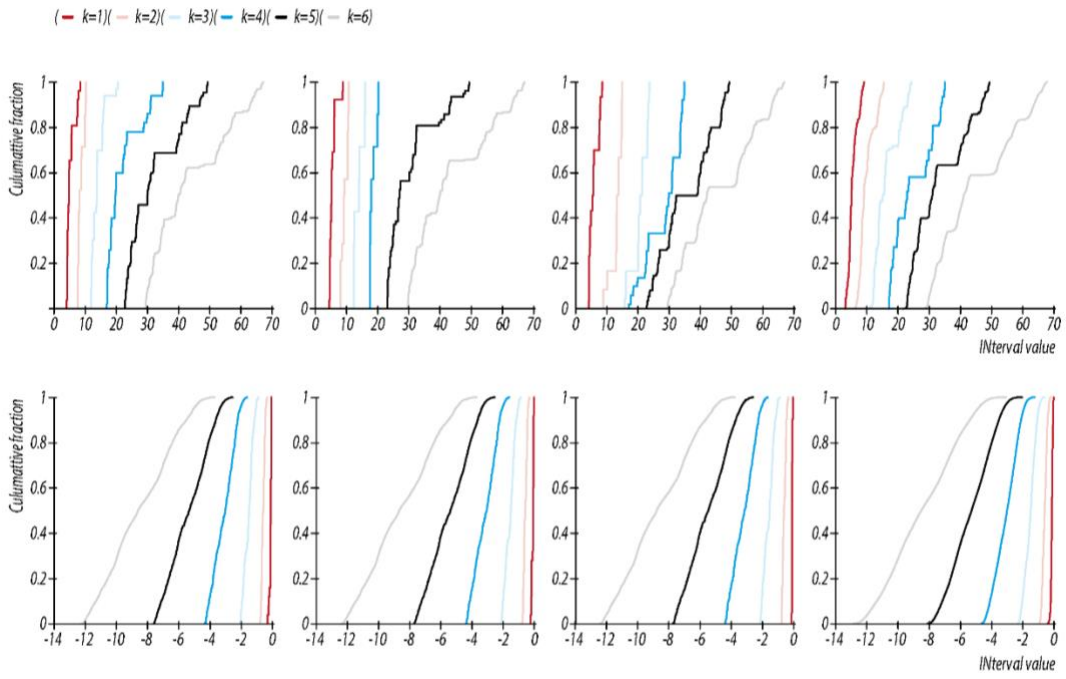

Figure S4: Time-Like and Spacelike Dendrogram Interval Values for the Positive Spacelike Signature Parameter Space This figure explores the interval values for time-like and spacelike dendrograms in the context of the positive spacelike signature parameter space. The figure is divided into several panels, each representing different aspects of the analysis.**Top row first 3 panels from the left: Cumulative Distribution Functions (cdfs) of Interval Values for Spacelike Dendrograms** depict the cumulative distribution functions (cdfs) of INterval values for spacelike dendrograms, focusing on three specific initial dendrograms at the initial level n=6 and varying k values (k=1, 2, ..., 6). Each panel showcases the distribution of interval values for spacelike dendrograms resulting from the transformation and branching processes. **Top row panel on the right: Cumulative Distribution Function (cdfs) of Interval Values for All Spacelike Dendrograms** presents the cumulative distribution function (cdfs) of INterval values for spacelike dendrograms, encompassing all initial dendrograms at the initial level n=6 and for each k value (k=1, 2, ..., 6). The visualization offers an overall perspective of the interval value distributions across all spacelike dendrograms.**Bottom row first 3 panels from the left: Cumulative Distribution Functions (cdfs) of Interval Values for Time-Like Dendrograms** illustrate the cumulative distribution functions (cdfs) of INterval values for time-like dendrograms, focusing on three specific initial dendrograms at the initial level n=6 and varying k values (k=1, 2, ..., 6). Each panel provides insights into the distribution of interval values for time-like dendrograms resulting from the transformation and branching processes. **Bottom row panel on the right: Cumulative Distribution Function (cdfs) of Interval Values for All Time-Like Dendrograms** displays the cumulative distribution function (cdfs) of INterval values for time-like dendrograms, encompassing all initial dendrograms at the initial level n=6 and for each k value (k=1, 2, ..., 6). The visualization presents an overall perspective of the INterval value distributions across all time-like dendrograms.